Electronic Supplementary Material (ESI) for Materials Advances.

Distortion Induced Structural Characteristics of $Ba_2R_{2/3}TeO_6$ (R =Y, Gd, Tb, Dy, Ho, Er, Tm, Yb and Lu) Double Perovskites and its Multifunctional Optical Properties in Lighting and Ratiometric Temperature Sensing

Sariga C. Lal, Jawahar I. N, Subodh G.[a*]

[a]Department of Physics, University of Kerala, Thiruvananthapuram, Kerala, India - 695581.

*e-mail: gsubodh@gmail.com

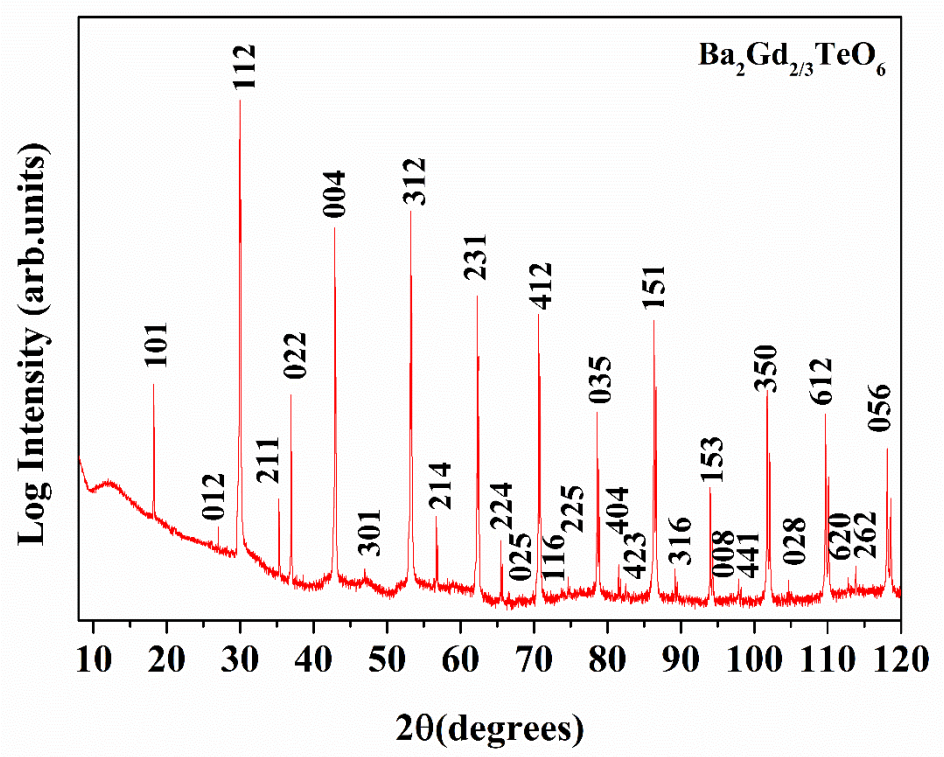

Figure SI 1. XRD pattern of $Ba_2Gd_{2/3}TeO_6$ indexed with monoclinic lattice planes.

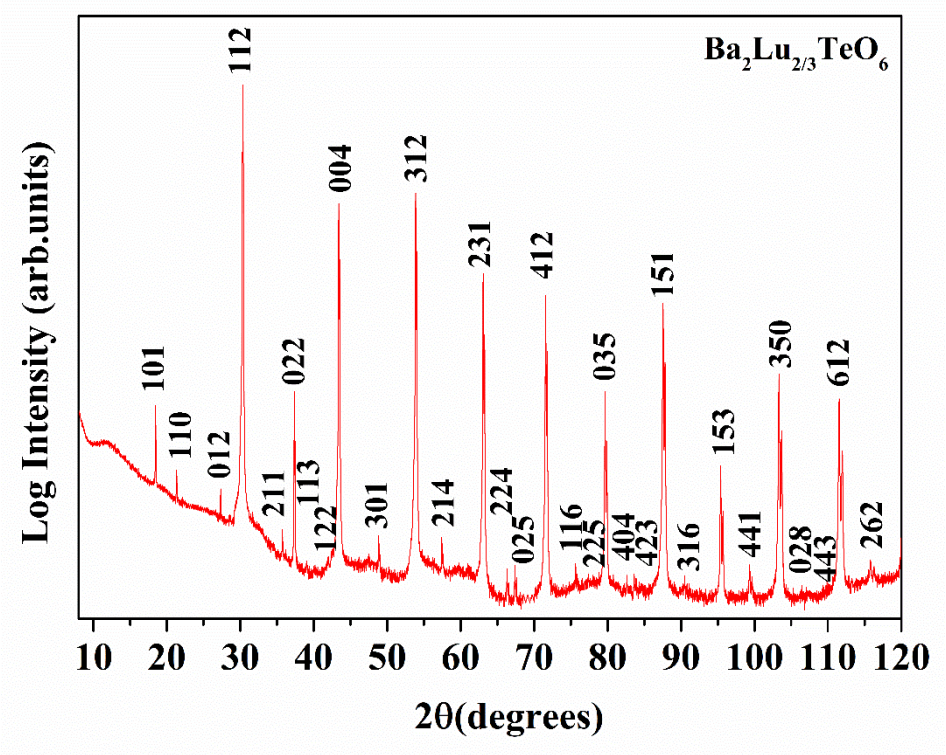

Figure SI 2. XRD pattern of $Ba_2Lu_{2/3}TeO_6$ indexed with monoclinic lattice planes.

Table SI 3. Tolerance factor of $Ba_2R_{2/3}TeO_6$ (R =La, Pr, Nd, Sm, Eu, Y, Gd, Tb, Dy, Ho, Er, Tm, Yb, Lu)

Compound	Tolerance factor
$Ba_2La_{2/3}TeO_6$	0.9692
$Ba_2Pr_{2/3}TeO_6$	0.9786
$Ba_2Nd_{2/3}TeO_6$	0.9801
$Ba_2Sm_{2/3}TeO_6$	0.9858
$Ba_2Eu_{2/3}TeO_6$	0.9883
$Ba_2Gd_{2/3}TeO_6$	0.9904
$Ba_2Tb_{2/3}TeO_6$	0.9938
$Ba_2Dy_{2/3}TeO_6$	0.9964
$Ba_2Ho_{2/3}TeO_6$	0.9990
$Ba_2Y_{2/3}TeO_6$	0.9992
$Ba_2Er_{2/3}TeO_6$	1.0015
$Ba_2Tm_{2/3}TeO_6$	1.0039
$Ba_2Yb_{2/3}TeO_6$	1.0068
$Ba_2Lu_{2/3}TeO_6$	1.0084

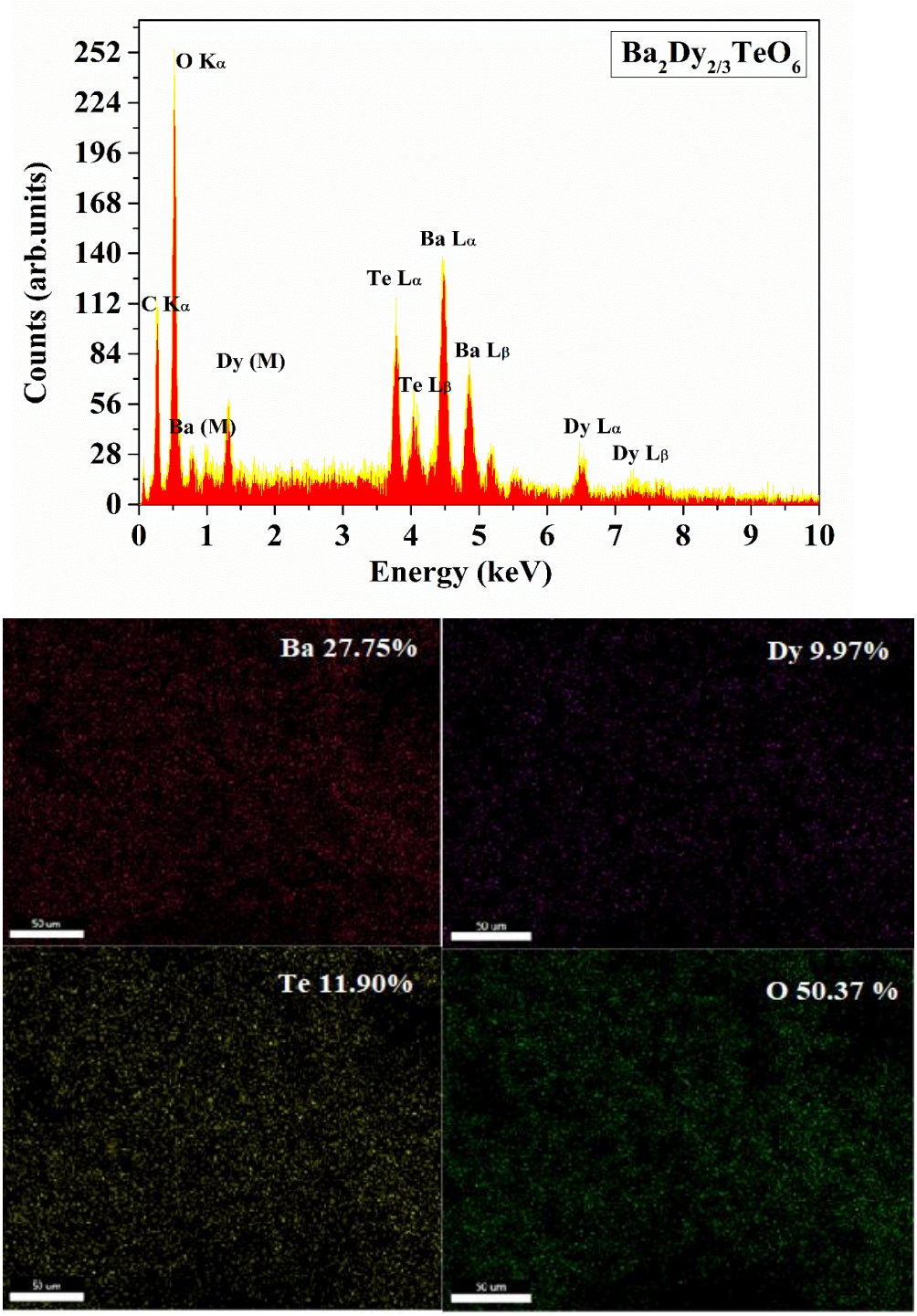

Figure SI 4. a) EDS of and b) Elemental mapping $Ba_2Dy_{2/3}TeO_6$.

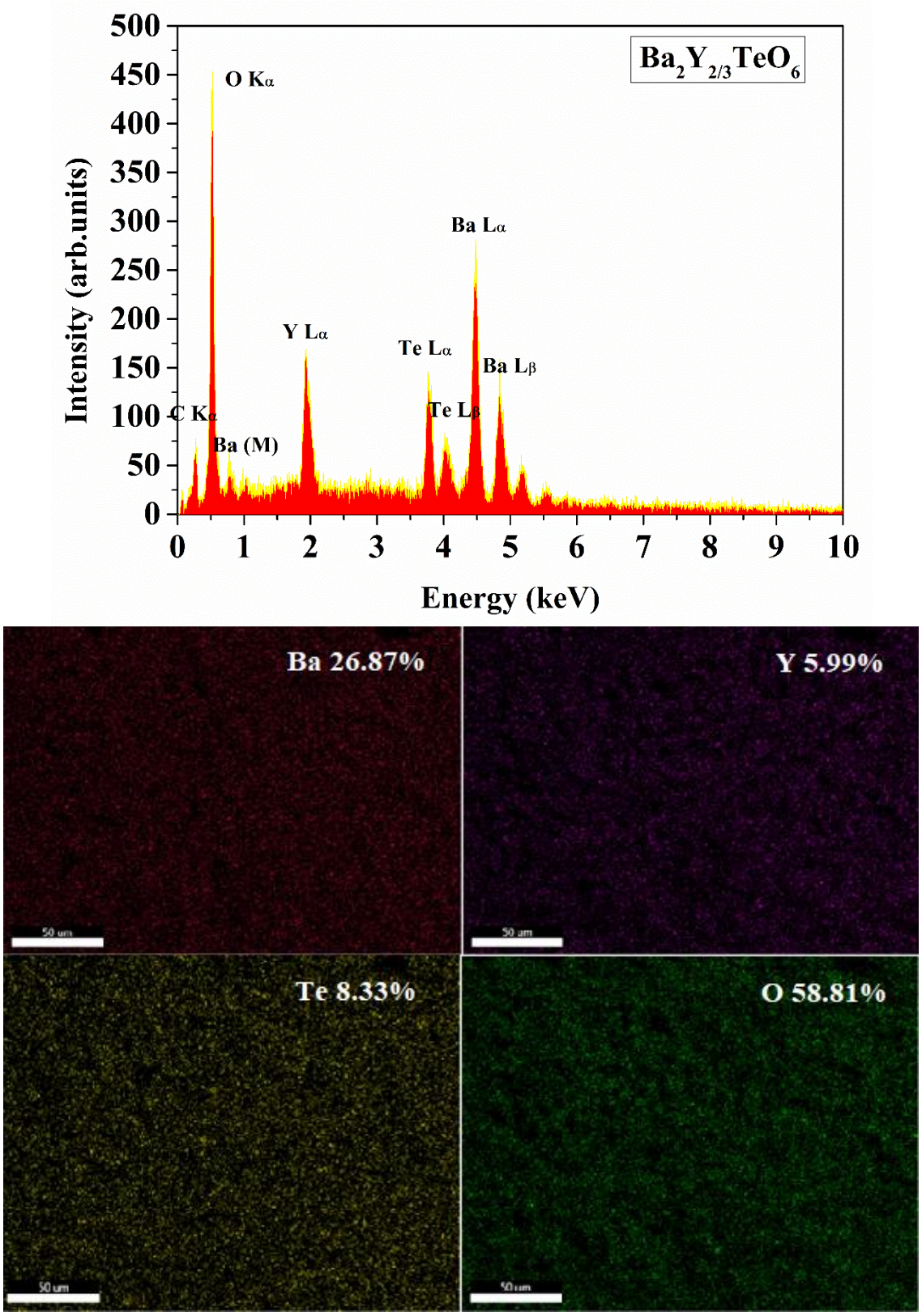

Figure SI 5. a) EDS of and b) Elemental mapping $Ba_2Y_{2/3}TeO_6$.

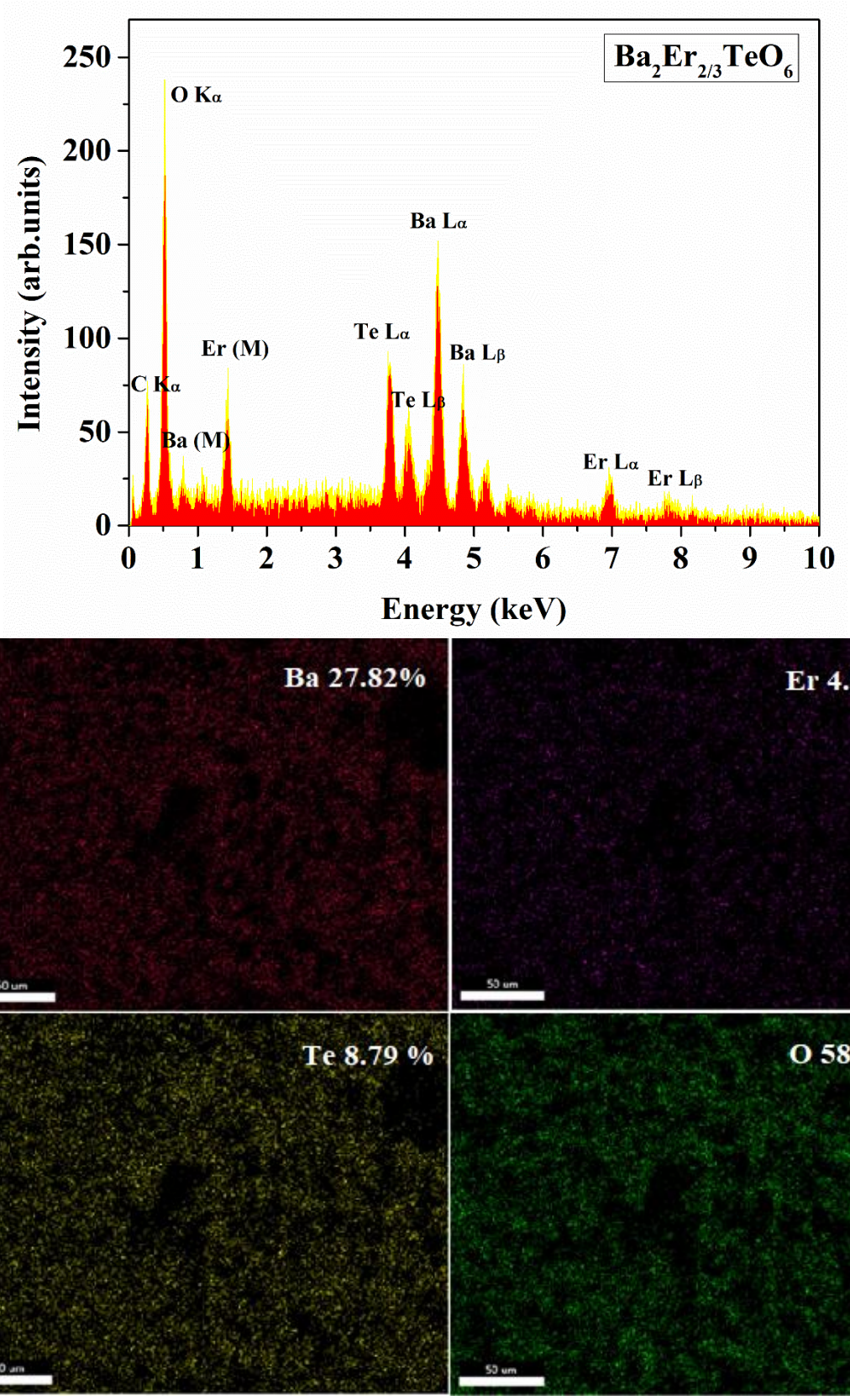

Figure SI 6. a) EDS of and b) Elemental mapping $Ba_2Er_{2/3}TeO_6$.

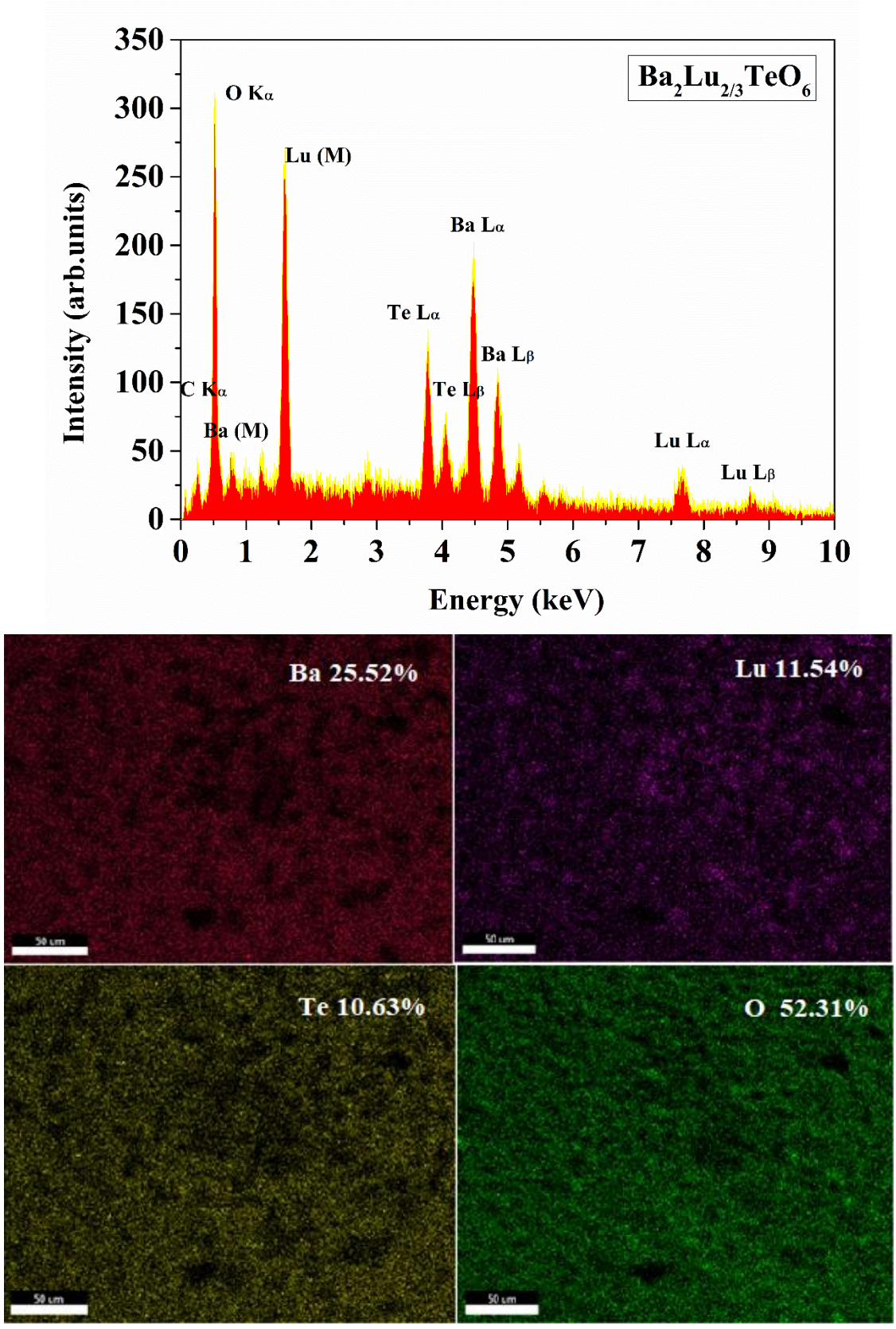

Figure SI 7. a) EDS of and b) Elemental mapping $Ba_2Lu_{2/3}TeO_6$.

Table SI 8: Atomic Percentage of $Ba_2R_{2/3}TeO_6$ (R = Gd, Dy, Y, Er, Lu) and $Ba_2Y_{2/3}TeO_6$: 10% Eu^{3+}.

Double Perovskites	Elements	Atomic % (%)
$Ba_2Gd_{2/3}TeO_6$	**Ba**	28.52
	Gd	9.52
	Te	12.33
	O	49.63
$Ba_2Dy_{2/3}TeO_6$	**Ba**	27.75
	Dy	9.97
	Te	11.90
	O	50.37
$Ba_2Y_{2/3}TeO_6$	**Ba**	26.87
	Y	5.99
	Te	8.33
	O	58.81
$Ba_2Er_{2/3}TeO_6$	**Ba**	27.82
	Er	4.55
	Te	8.79
	O	58.84
$Ba_2Lu_{2/3}TeO_6$	**Ba**	25.52
	Lu	11.54
	Te	10.63
	O	52.31
$Ba_2Y_{2/3}TeO_6$: 10% Eu^{3+}	**Ba**	29.42
	Y	3.98
	Eu	2.01
	Te	12.10
	O	52.49

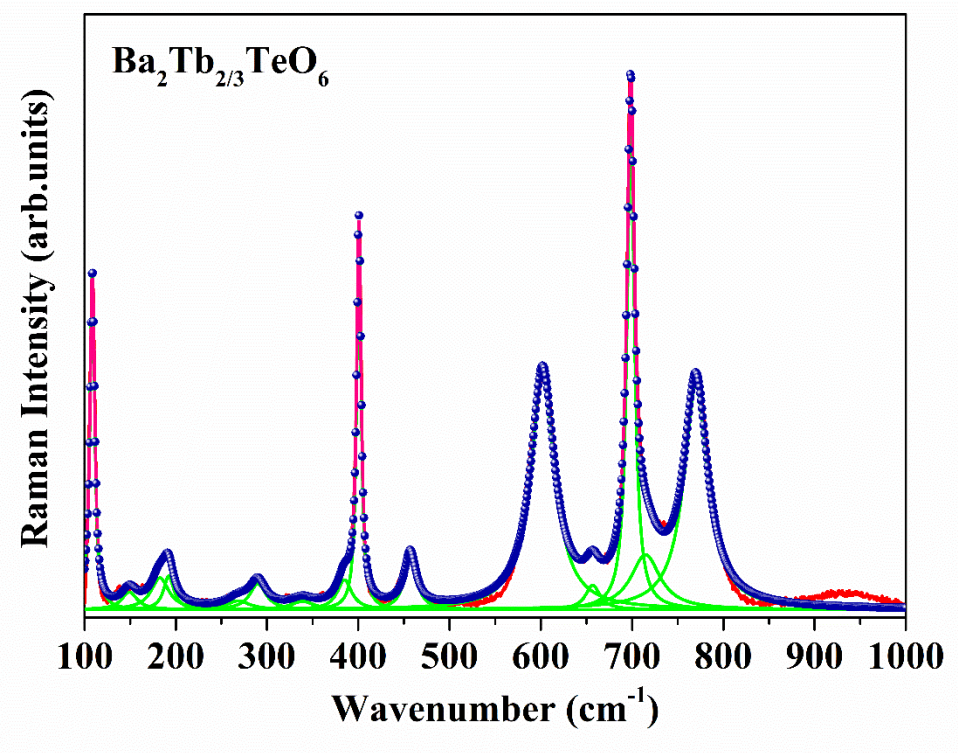

Figure SI 9. Deconvoluted Raman spectrum of $Ba_2Tb_{2/3}TeO_6$.

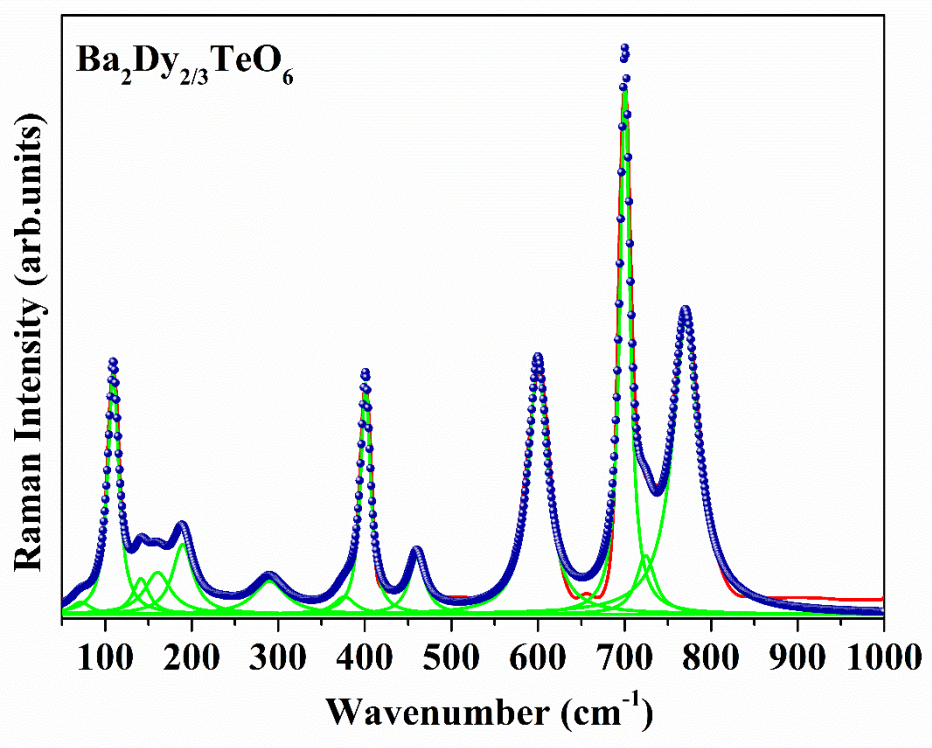

Figure SI 10. Deconvoluted Raman spectrum of $Ba_2Dy_{2/3}TeO_6$.

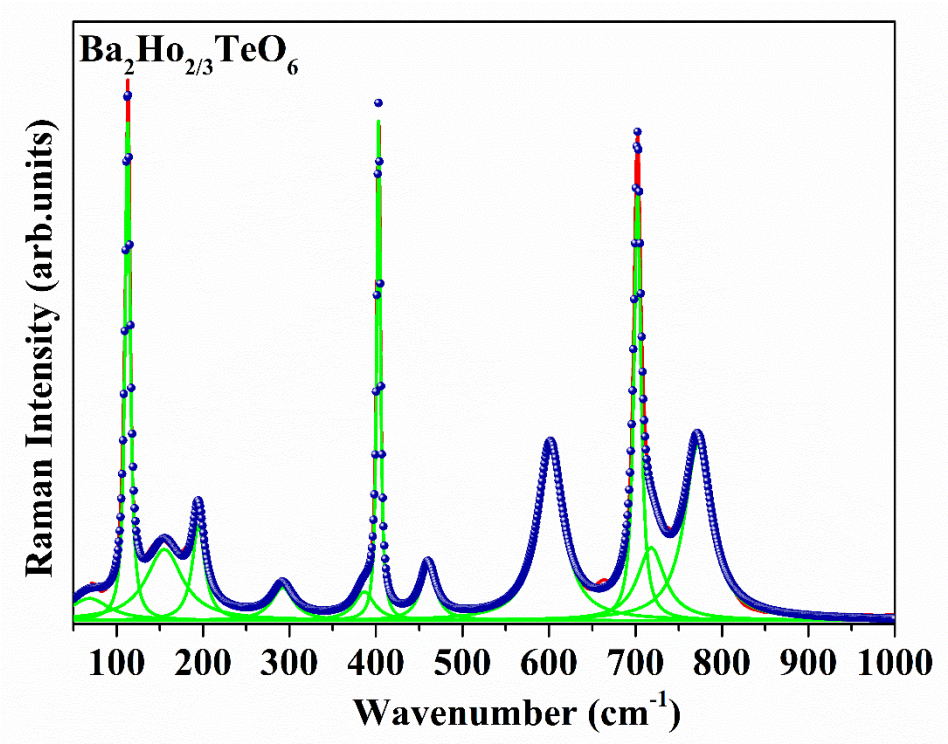

Figure SI 11. Deconvoluted Raman spectrum of $Ba_2Ho_{2/3}TeO_6$.

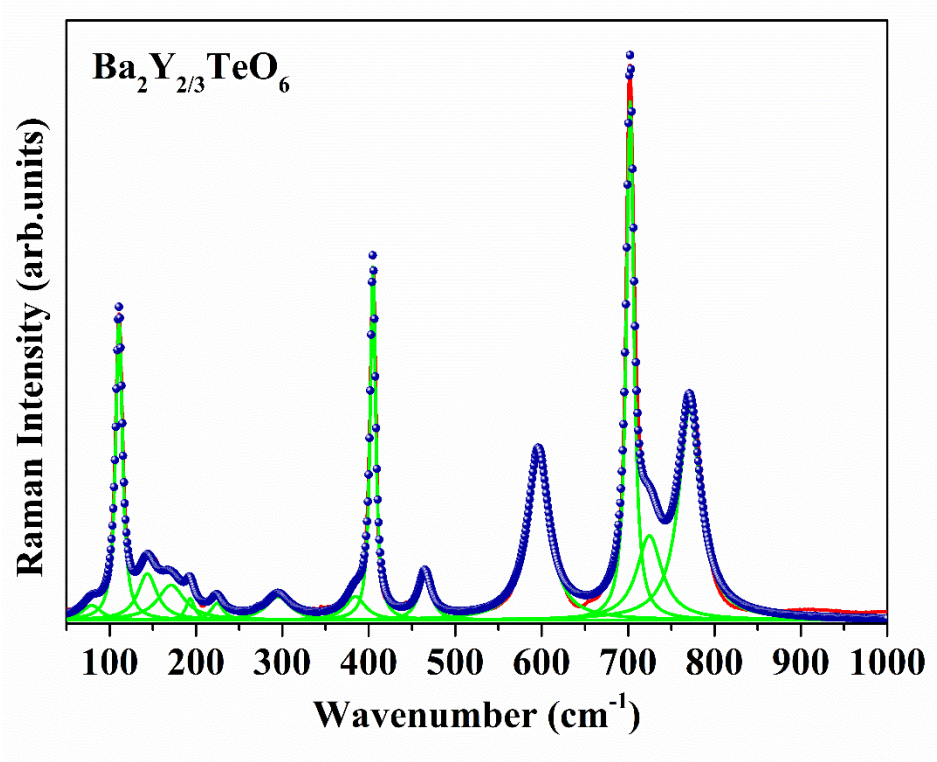

Figure SI 12. Deconvoluted Raman spectrum of $Ba_2Y_{2/3}TeO_6$.

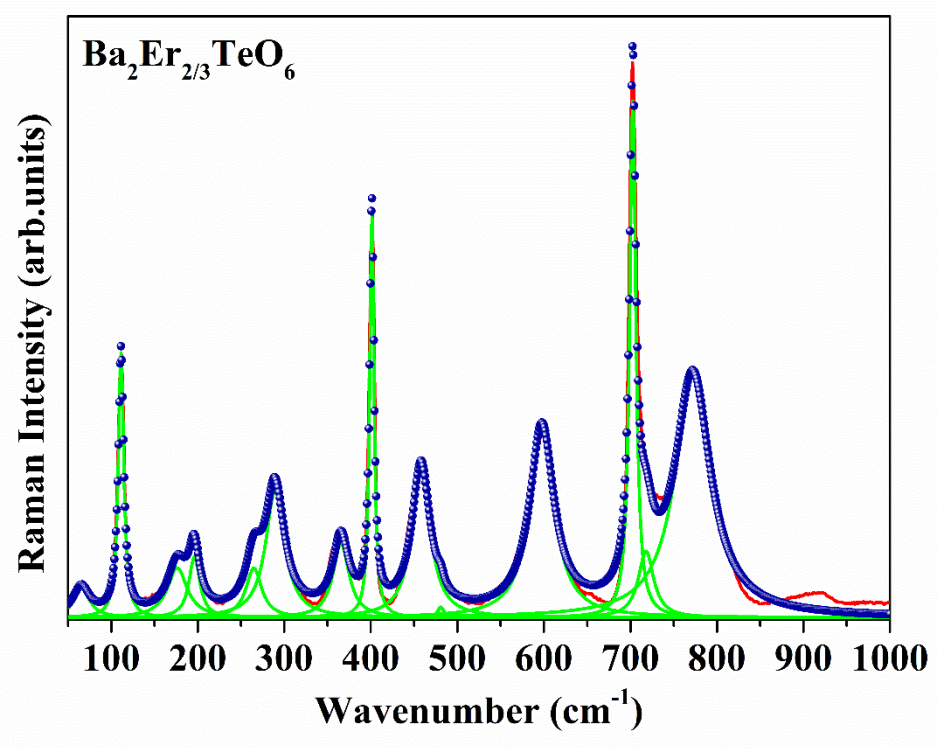

Figure SI 13. Deconvoluted Raman spectrum of $Ba_2Er_{2/3}TeO_6$.

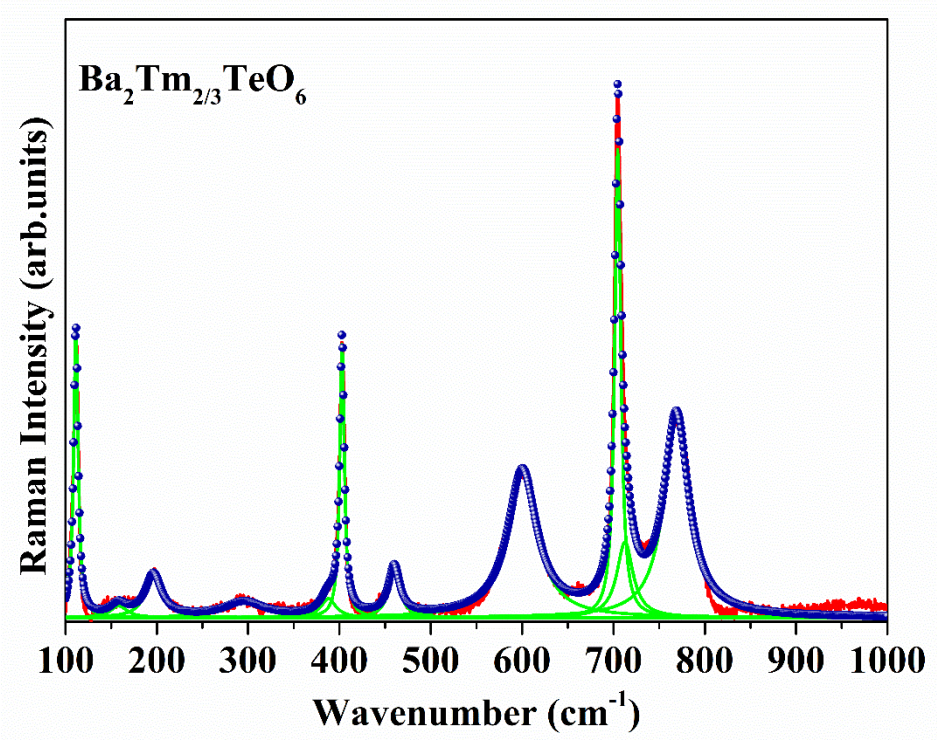

Figure SI 14. Deconvoluted Raman spectrum of $Ba_2Tm_{2/3}TeO_6$.

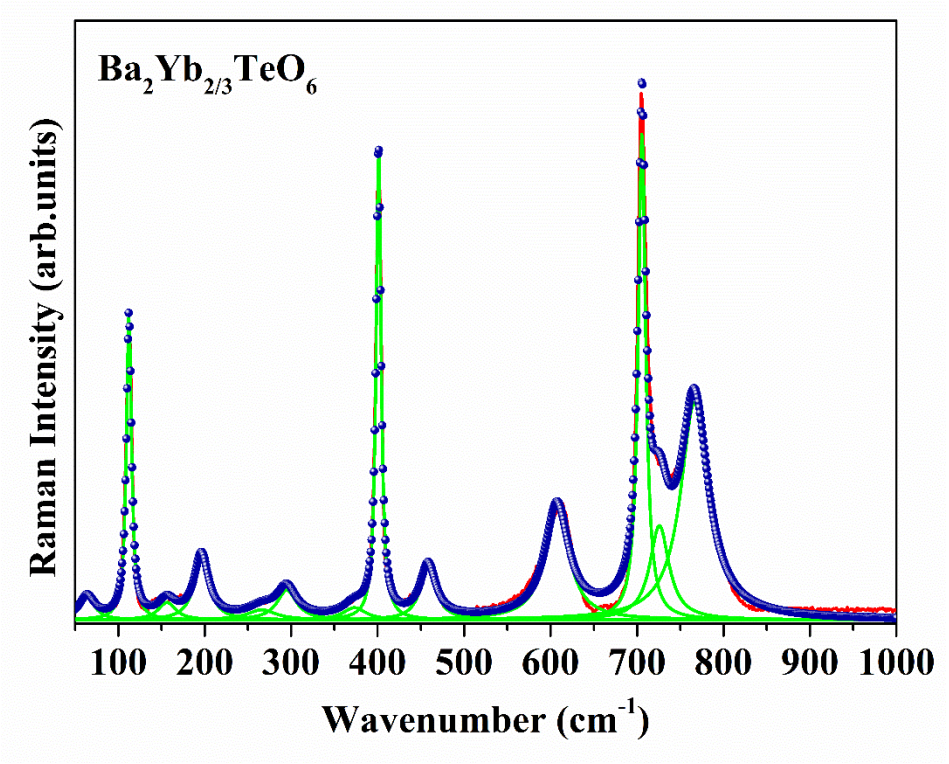

Figure SI 15. Deconvoluted Raman spectrum of $Ba_2Yb_{2/3}TeO_6$.

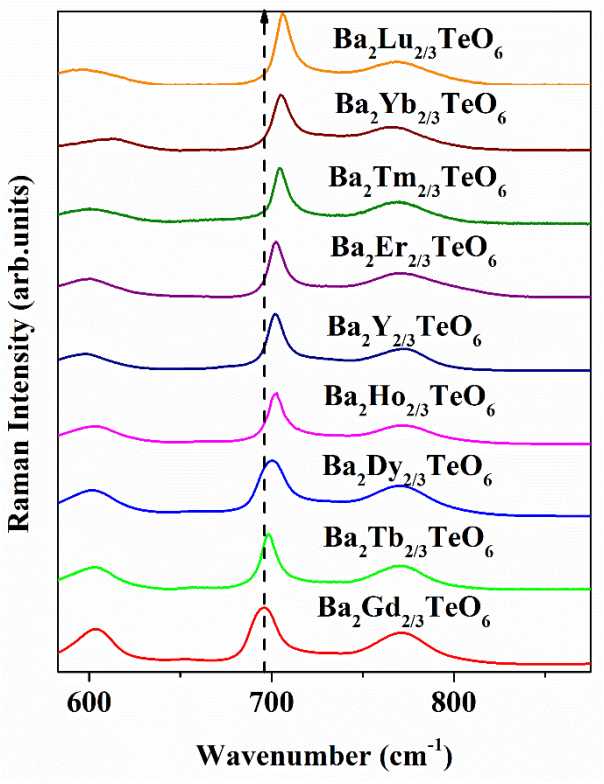

Figure SI 16. Shift in Raman modes above 650 cm^{-1}.

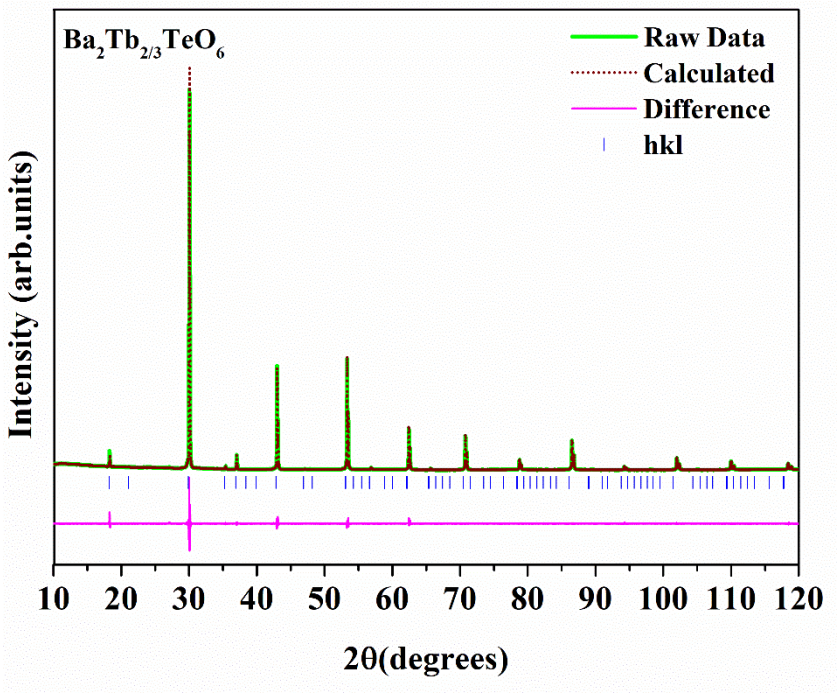

Figure SI 17. Rietveld refinement of XRD pattern of $Ba_2Tb_{2/3}TeO_6$.

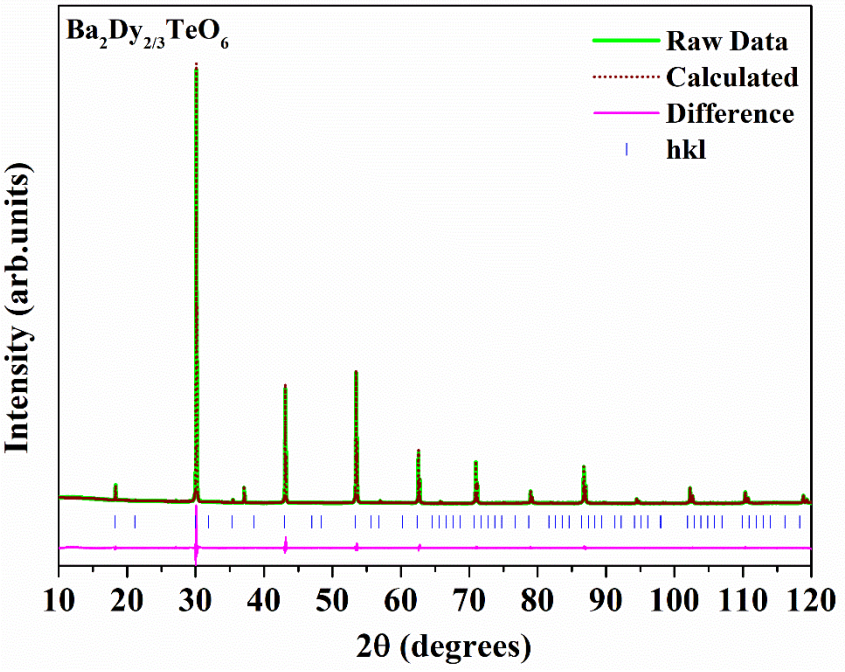

Figure SI 18. Rietveld refinement of XRD pattern of $Ba_2Dy_{2/3}TeO_6$.

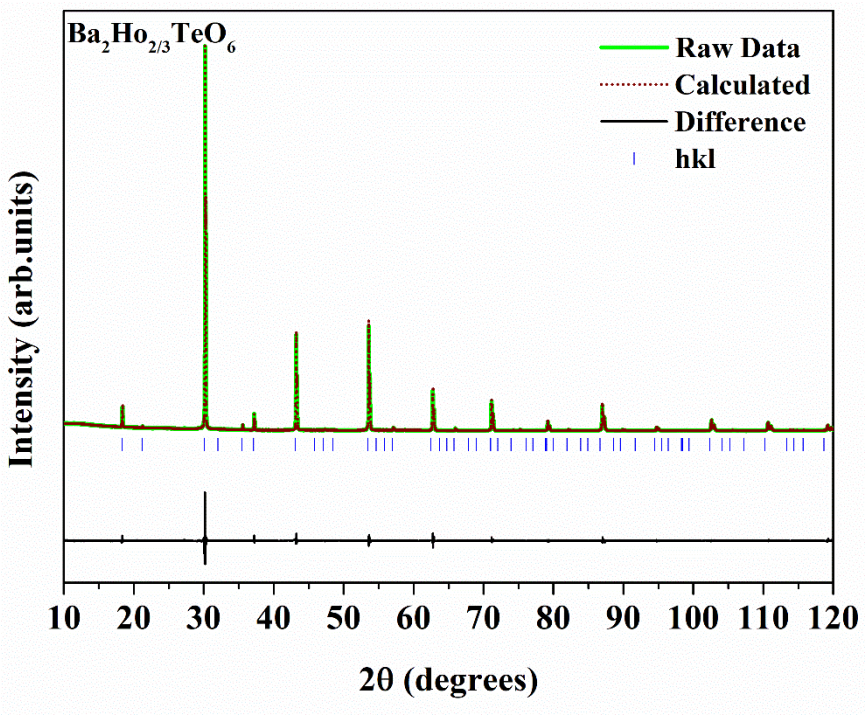

Figure SI 19. Rietveld refinement of XRD pattern of $Ba_2Ho_{2/3}TeO_6$.

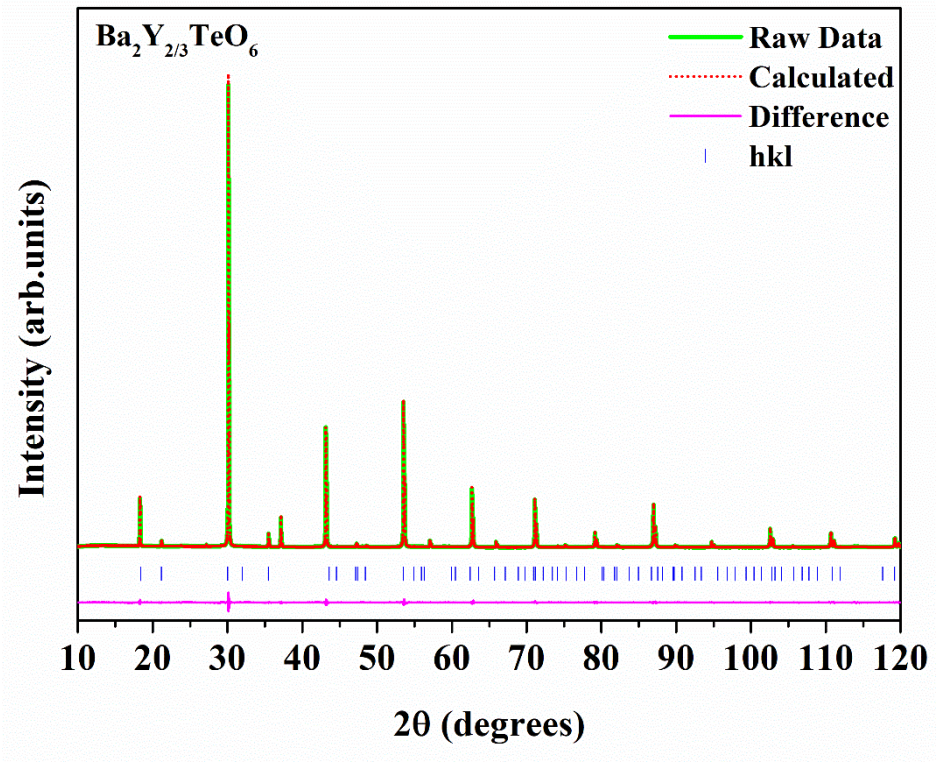

Figure SI 20. Rietveld refinement of XRD pattern of $Ba_2Y_{2/3}TeO_6$.

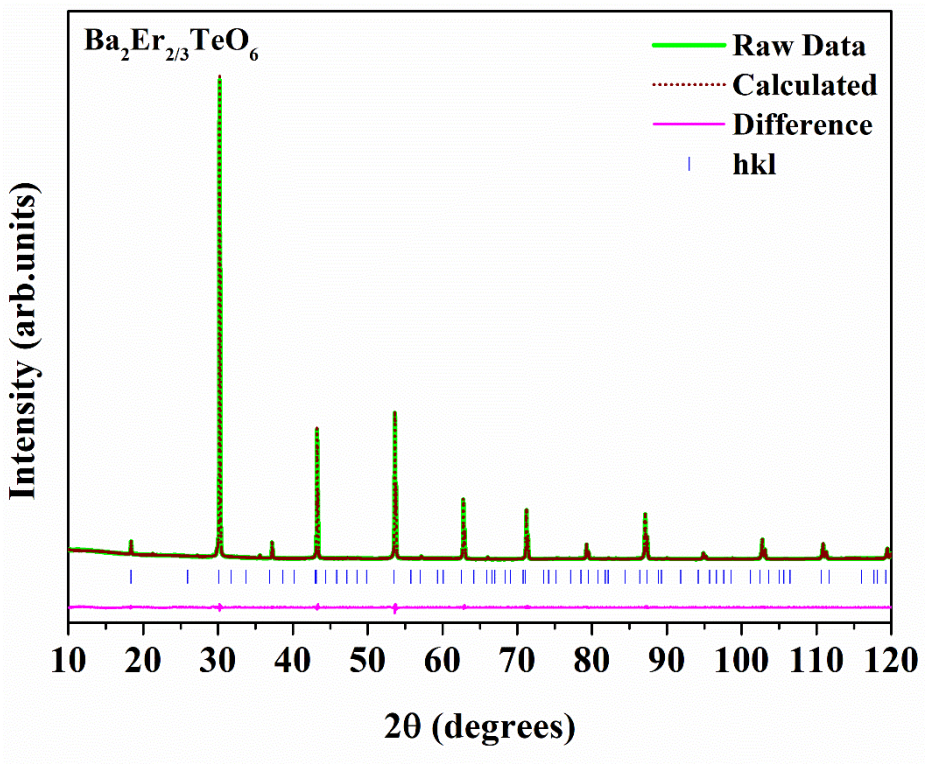

Figure SI 21. Rietveld refinement of XRD pattern of $Ba_2Er_{2/3}TeO_6$.

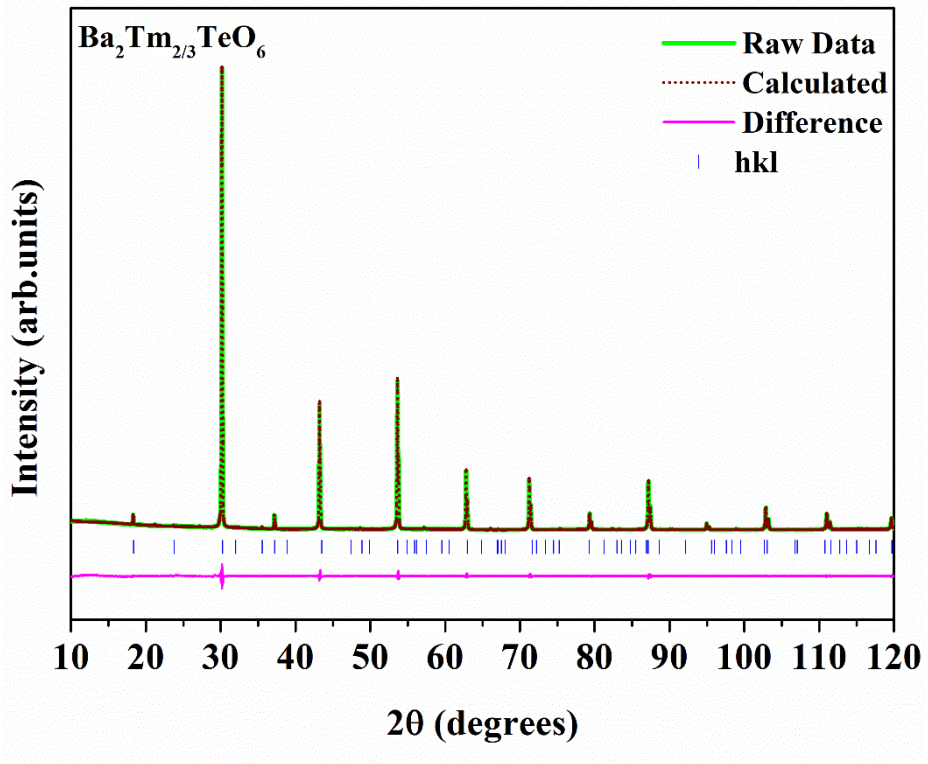

Figure SI 22. Rietveld refinement of XRD pattern of $Ba_2Tm_{2/3}TeO_6$.

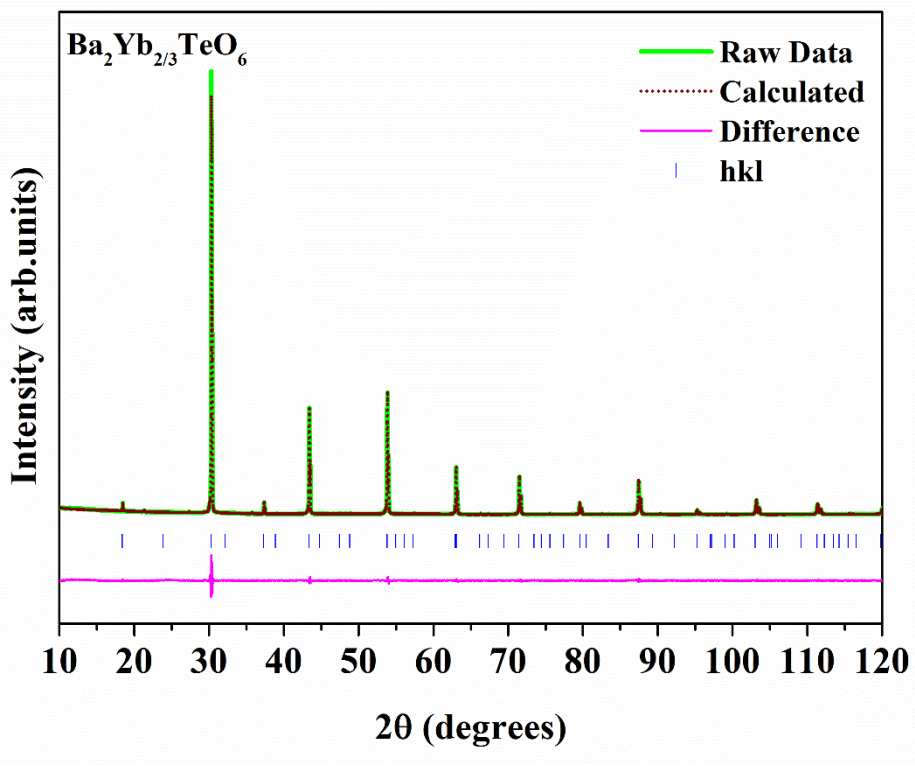

Figure SI 23. Rietveld refinement of XRD pattern of $Ba_2Yb_{2/3}TeO_6$.

Table SI 24. Refinement parameters of $Ba_2R_{2/3}TeO_6$ (R = Tb, Dy, Ho,Y, Er, Tm, Yb)

$Ba_2Tb_{2/3}TeO_6$						
a = 5.9695(5) Å		*b = 5.9595(5) Å*		*c = 8.4655(1) Å*		*β = 90.0145°*
R_{exp} = 1.96%		*R_{wp} = 5.25%*		*R_p= 3.17%*		*GOF = 2.68*
Ions	Wyckoff sites	x	y	z	Occupancy	B_{eq}(Å^2)
Ba	4e	0.490(6)	0.519(5)	0.257(7)	1	0.90(9)
Tb	2d	0.5	0	0	0.667	0.40(5)
Te	2c	0	0.5	0	1	0.40(5)
O1	4e	0.215(5)	0.251(4)	0.013(1)	1	0.98(8)
O2	4e	0.200(5)	0.771(6)	0.004(5)	1	0.98(2)
O3	4e	0.499(9)	0.016(6)	0.264(3)	1	0.97(3)
$Ba_2Dy_{2/3}TeO_6$						
a = 5.9557(4) Å		*b = 5.9474(7) Å*		*c = 8.3920(1) Å*		*β = 90.0141°*
R_{exp} = 1.88%		*R_{wp} = 5.36%*		*R_p= 3.61%*		*GOF = 2.85*
Ions	Wyckoff sites	x	y	z	Occupancy	B_{eq}(Å^2)
Ba	4e	0.496(1)	0.501(9)	0.257(6)	1	0.92(6)
Dy	2d	0.5	0.	0	0.667	0.46(3)
Te	2c	0	0.5	0	1	0.46(3)
O1	4e	0.215(5)	0.251(4)	0.008(1)	1	0.96(8)
O2	4e	0.200(5)	0.771(6)	0.004(1)	1	0.98(1)
O3	4e	0.505(6)	0.016(6)	0.264(3)	1	0.95(3)
$Ba_2Ho_{2/3}TeO_6$						
a = 5.9246(1) Å		*b = 5.9330(6) Å*		*c = 8.3837(1) Å*		*β = 90.0136°*
R_{exp} = 3.57%		*R_{wp} = 7.94%*		*R_p= 5.45%*		*GOF = 2.22*
Ions	Wyckoff sites	x	y	z	Occupancy	B_{eq}(Å^2)

Ba	4e	0.498(8)	0.501(9)	0.257(6)	1	0.91(6)
Ho	2d	0.5	0.	0	0.667	0.45(3)
Te	2c	0	0.5	0	1	0.45(3)
O1	4e	0.215(5)	0.251(4)	0.006(1)	1	0.95(8)
O2	4e	0.200(5)	0.771(6)	0.003(1)	1	0.98(1)
O3	4e	0.501(4)	0.016(6)	0.264(3)	1	0.94(3)

$Ba_2Y_{2/3}TeO_6$

a = 5.9223(1) Å *b = 5.9309(6) Å* *c = 8.3880(9) Å* *β = 90.0115°*

R_{exp} *= 3.34%* R_{wp} *= 5.21%* R_p *= 3.90%* *GOF = 1.56*

Ions	Wyckoff sites	x	y	z	Occupancy	B_{eq}(Å^2)
Ba	4e	0.497(1)	0.520(5)	0.257(1)	1	0.93(5)
Y	2d	0.5	0.	0	0.667	0.47(3)
Te	2c	0	0.5	0	1	0.47(3)
O1	4e	0.215(5)	0.251(4)	0.009(1)	1	0.93(8)
O2	4e	0.200(5)	0.771(6)	0.001(1)	1	0.96(1)
O3	4e	0.476(8)	0.016(6)	0.264(3)	1	0.92(3)

$Ba_2Er_{2/3}TeO_6$

a = 5.9220(6) Å *b = 5.9165(5) Å* *c = 8.3748(5) Å* *β = 90.0115°*

R_{exp} *= 2.11%* R_{wp} *= 3.74%* R_p *= 2.89%* *GOF = 1.77*

Ions	Wyckoff sites	x	y	z	Occupancy	B_{eq}(Å^2)
Ba	4e	0.487(8)	0.501(4)	0.257(1)	1	0.95(5)
Er	2d	0.5	0.	0	0.667	0.50(3)
Te	2c	0	0.5	0	1	0.50(3)
O1	4e	0.215(5)	0.251(4)	0.008(9)	1	0.93(5)
O2	4e	0.200(5)	0.771(6)	0.001(9)	1	0.98(1)
O3	4e	0.497(9)	0.016(6)	0.264(3)	1	0.92(1)

$Ba_2Tm_{2/3}TeO_6$

a = 5.9224(4) Å	*b = 5.9169(4) Å*	*c = 8.3728(4) Å*	*β = 90.0105°*
R_{exp} = 2.04%	*R_{wp} = 4.40%*	*R_p=3.49%*	*GOF = 2.16*

Ions	Wyckoff sites	x	y	z	Occupancy	B_{eq}(Å^2)
Ba	4e	0.509(3)	0.521(5)	0.257(1)	1	0.97(5)
Tm	2d	0.5	0.	0	0.667	0.55(3)
Te	2c	0	0.5	0	1	0.55(3)
O1	4e	0.215(5)	0.251(4)	0.008(4)	1	0.89(5)
O2	4e	0.200(5)	0.771(6)	0.001(9)	1	0.94(1)
O3	4e	0.507(8)	0.016(6)	0.264(3)	1	0.87(1)

$Ba_2Yb_{2/3}TeO_6$

a = 5.9090(1) Å	*b = 5.9169(9) Å*	*c = 8.3474(6) Å*	*β = 90.0111°*
R_{exp} = 2.92%	*R_{wp} = 7.02%*	*R_p= 5.41%*	*GOF = 2.40*

Ions	Wyckoff sites	x	y	z	Occupancy	B_{eq}(Å^2)
Ba	4e	0.501(6)	0.505(1)	0.256(9)	1	0.98(5)
Yb	2d	0.5	0.	0	0.667	0.60(3)
Te	2c	0	0.5	0	1	0.60(1)
O1	4e	0.215(5)	0.251(4)	0.008(4)	1	0.87(5)
O2	4e	0.200(5)	0.771(6)	0.001(8)	1	0.92(5)
O3	4e	0.502(8)	0.016(6)	0.264(3)	1	0.85(5)

Table SI 25. Selected bond distances of $Ba_2R_{2/3}TeO_6$ (R = Tb, Dy, Ho, Y, Er, Tm, Yb).

Bonds	**Bond lengths (Å)**	**Bonds**	**Bond lengths (Å)**	**Bonds**	**Bond lengths (Å)**	**Bonds**	**Bond lengths (Å)**	**Bonds**	**Bond lengths (Å)**	**Bonds**	**Bond lengths (Å)**	**Bonds**	**Bond lengths (Å)**
Tb – O1	2.268	Dy – O1	2.261	Ho – O1	2.252	Y – O1	2.252	Er – O1	2.249	Tm –O1	2.249	Yb – O1	2.246
Tb – O2	2.252	Dy – O2	2.247	Ho – O2	2.237	Y – O2	2.236	Er – O2	2.234	Tm –O2	2.234	Yb – O2	2.231
Tb – O3	2.237	Dy – O3	2.218	Ho – O3	2.215	Y – O3	2.221	Er – O3	2.213	Tm –O3	2.213	Yb – O3	2.206
Te – O1	1.965	Te – O1	1.959	Te – O1	1.951	Te – O1	1.951	Te – O1	1.948	Te – O1	1.948	Te – O1	1.947
Te – O2	2.009	Te – O2	2.004	Te – O2	1.997	Te – O2	1.997	Te – O2	1.993	Te – O2	1.994	Te – O2	1.992
Te – O3	2.000	Te – O3	1.983	Te – O3	1.981	Te – O3	1.987	Te – O3	1.979	Te – O3	1.979	Te – O3	1.972

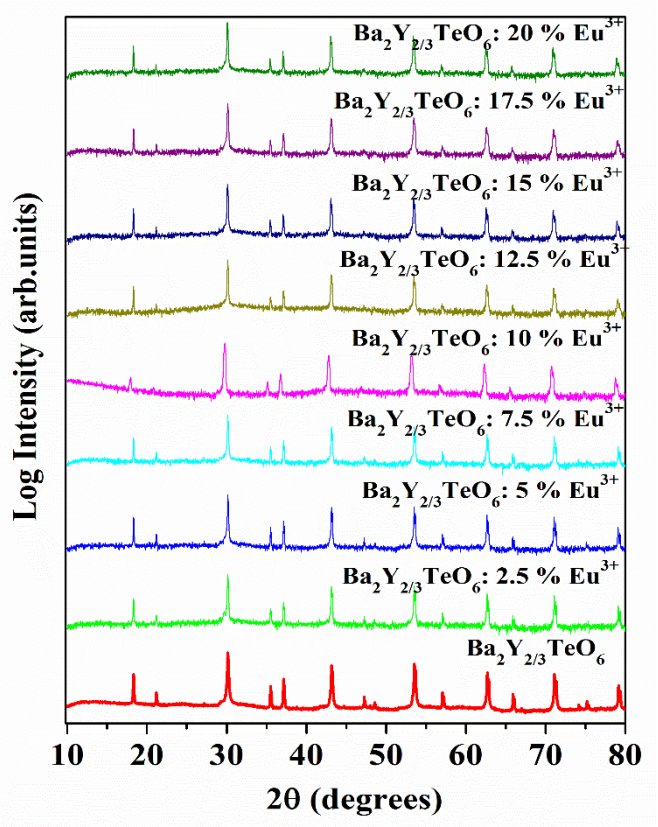

Figure SI 26. Combined XRD of $Ba_2Y_{2/3}TeO_6$: x% Eu^{3+} (x = 0, 2.5, 5, 7.5, 10, 12.5 15, 17.5 and 20).

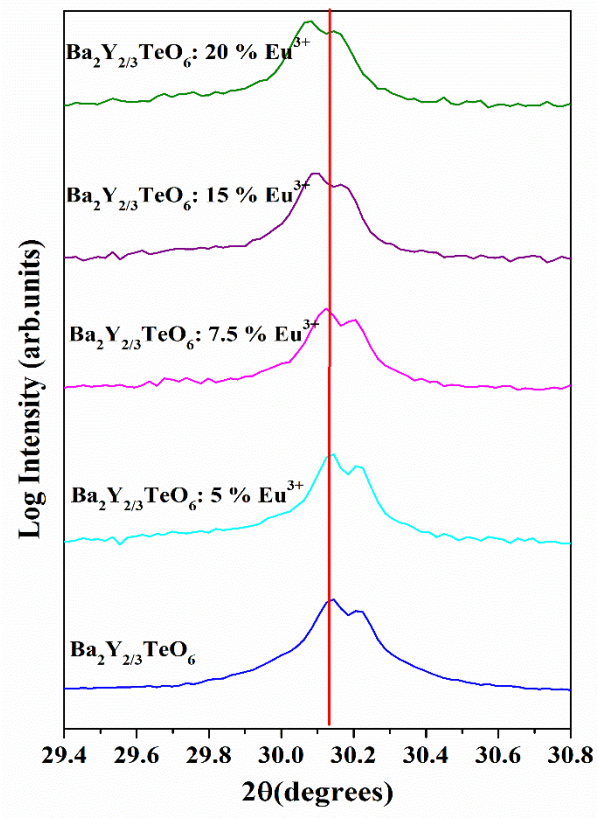

Figure SI 27. Shift of psuedocubic *220* reflection with Eu^{3+} concentration.

Table SI 28. Lattice parameters and cell volume of $Ba_2Y_{2/3}TeO_6$: Eu^{3+}.

Phosphor	a (Å)	b (Å)	c (Å)	β (°)	Cell Volume (Å^3)
$Ba_2Y_{2/3}TeO_6$	*5.9223(1)*	*5.9309(6)*	*8.3880(9)*	*90.0115*	*294.6249*
$Ba_2Y_{2/3}TeO_6$:5%Eu^{3+}	*5.9284(1)*	*5.9291(1)*	*8.3871(2)*	*90.0115*	*294.8072*
$Ba_2Y_{2/3}TeO_6$:7.5%Eu^{3+}	*5.9286(9)*	*5.9299(4)*	*8.3882(4)*	*90.0115*	*294.8955*
$Ba_2Y_{2/3}TeO_6$:15%Eu^{3+}	*5.9282(5)*	*5.9367(8)*	*8.3949(1)*	*90.0115*	*295.4496*
$Ba_2Y_{2/3}TeO_6$:20%Eu^{3+}	*5.9297(2)*	*5.9386(6)*	*8.3984(3)*	*90.0115*	*295.7422*

Table SI 29. Refinement parameters of $Ba_2Y_{2/3}TeO_6$: 10% Eu^{3+}.

a = 5.9223(1) Å		*b = 5.9320(4) Å*		*c = 8.3999(8) Å*	*β = 90.0115°*	
R_{exp} = 2.54%		*R_{wp} = 3.72%*		*R_p= 2.78%*	*GOF = 1.46*	
Ions	Wyckoff sites	x	y	z	Occupancy	B_{eq}(Å^2)
Ba	4e	0.492(5)	0.525(4)	0.257(1)	1	0.93(1)
Y	2d	0.5	0	0	0.567	0.47(3)
Eu	2d	0.5	0	0	0.1	0.47(3)
Te	2c	0	0.5	0	1	0.47(3)
O1	4e	0.215(5)	0.251(4)	0.008(5)	1	0.93(8)
O2	4e	0.200(5)	0.771(6)	0.001(6)	1	0.96(1)
O3	4e	0.481(5)	0.016(6)	0.264(3)		0.92 (3)

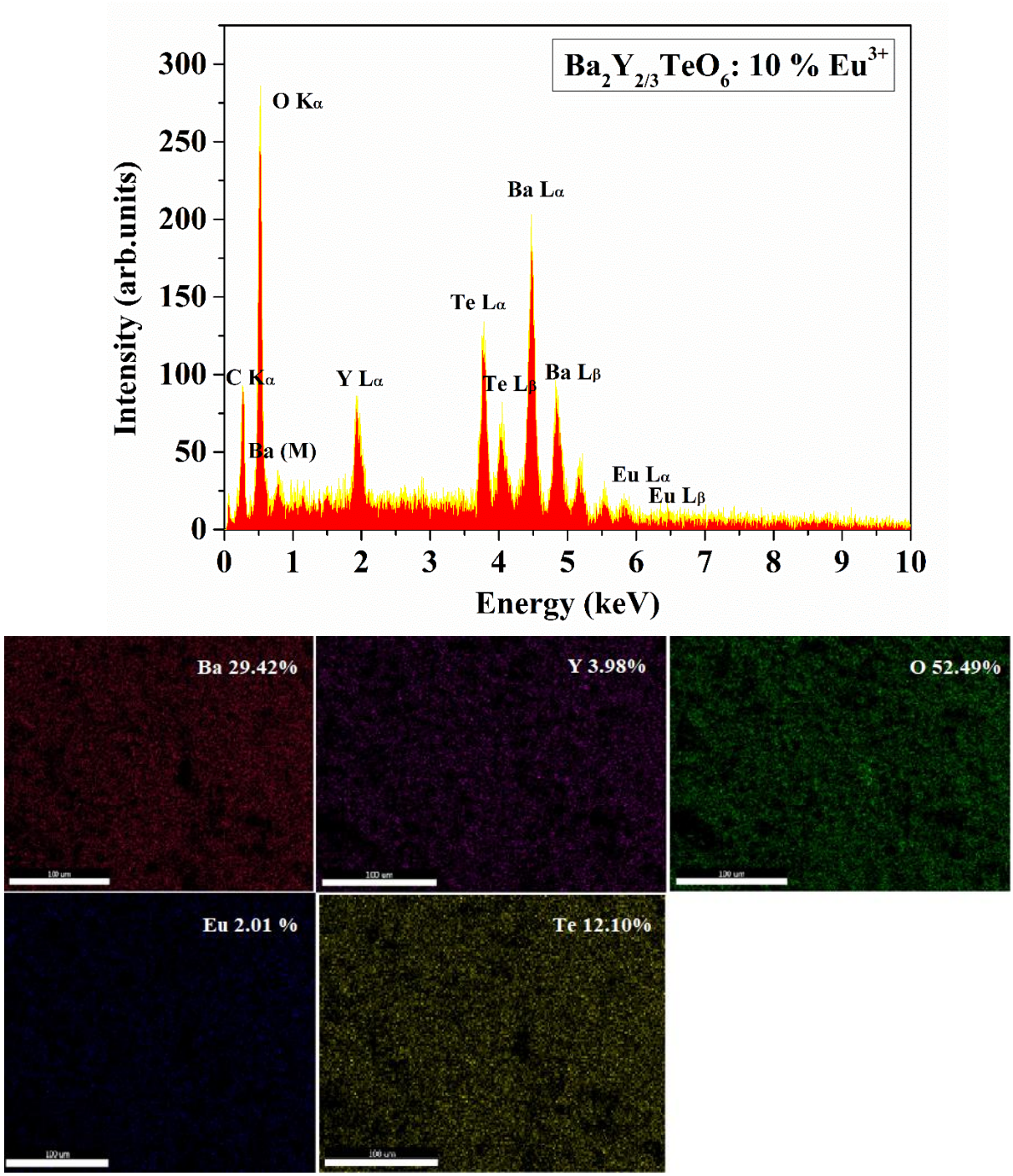

Figure SI 30. a) EDS of and b) Elemental mapping $Ba_2Y_{2/3}TeO_6$: 10% Eu^{3+}.

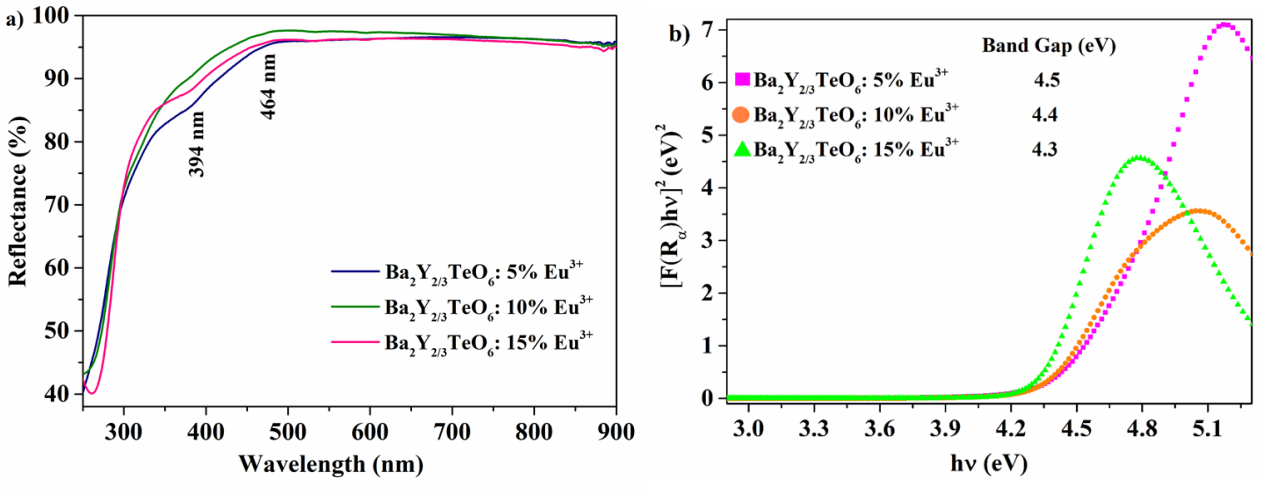

Figure SI 31. a) Diffuse reflectance spectra of $Ba_2Y_{2/3}TeO_6$: x% Eu^{3+}(x = 5, 10, 15%) and b) Kubelka Munk plot of hν vs $[F(R_\infty)h\nu]^2$ of $Ba_2Y_{2/3}TeO_6$: x% Eu^{3+} (x = 5, 10, 15 mol %).

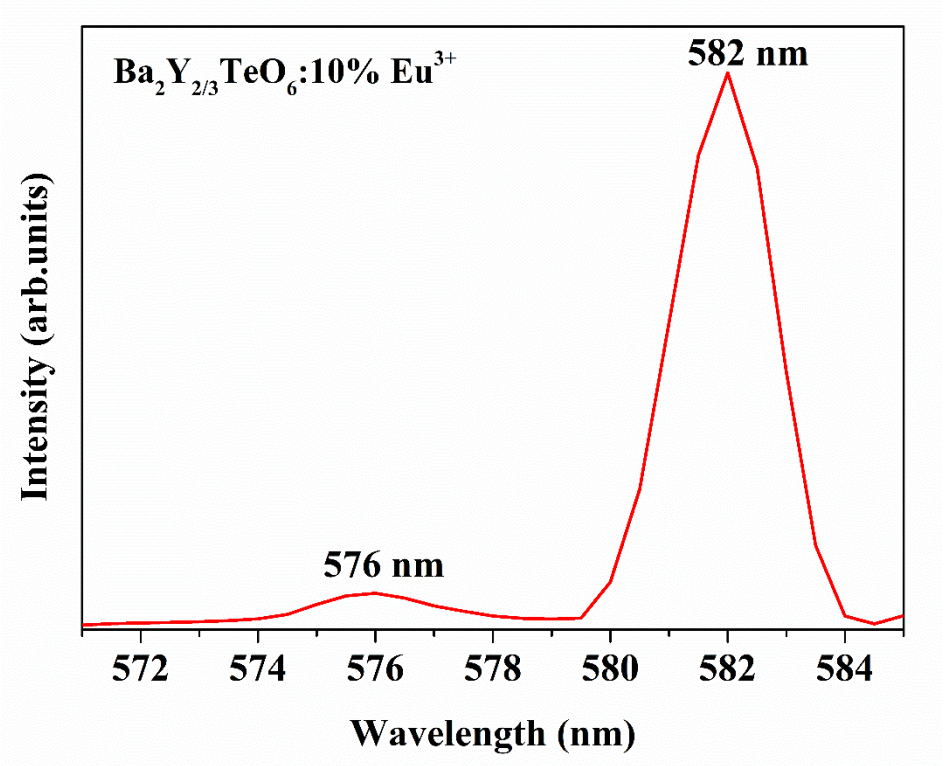

Figure SI 32. Emission spectrum with high spectral resolution in the region 570-585 nm.

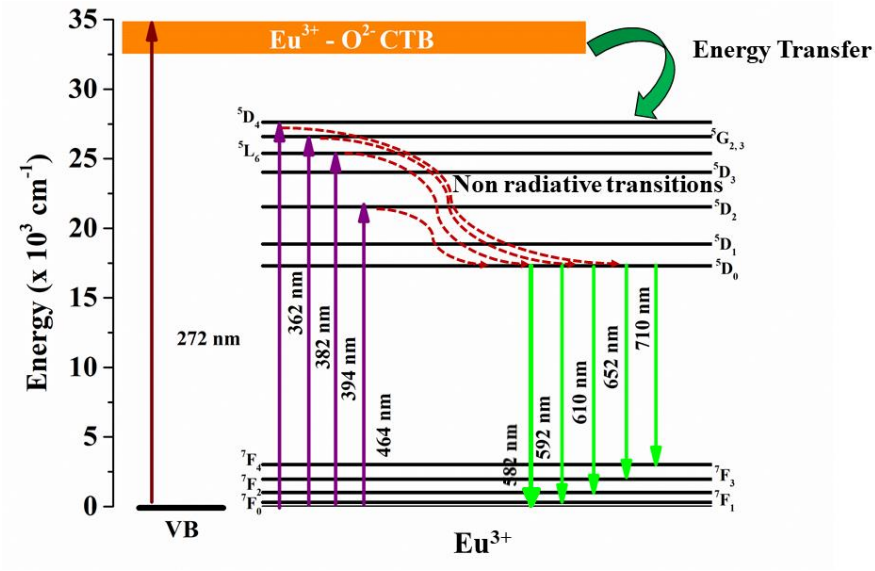

Figure SI 33. Photoluminescence mechanism in $Ba_2Y_{2/3}TeO_6$: Eu^{3+}.

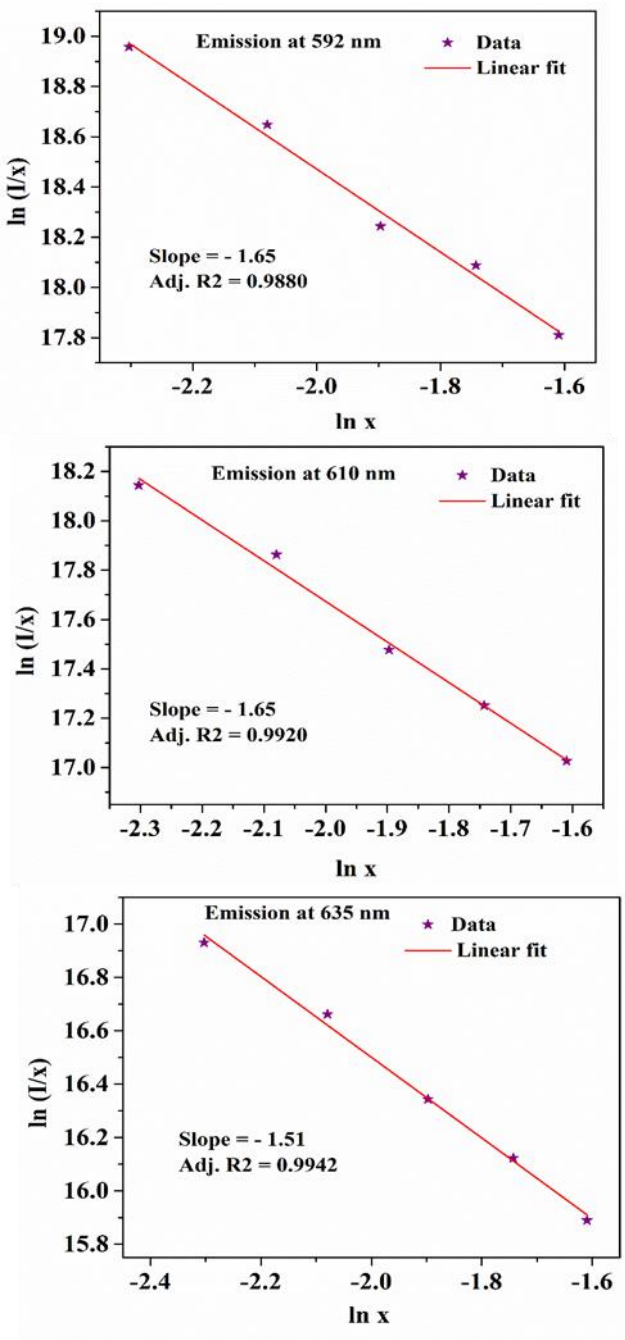

Figure SI 34. Plots of *ln x* vs *ln (I/x)* of $Ba_2Y_{2/3}TeO_6$: x% Eu^{3+} at different concentrations (x = 10, 12.5, 15, 17.5 and 20%).

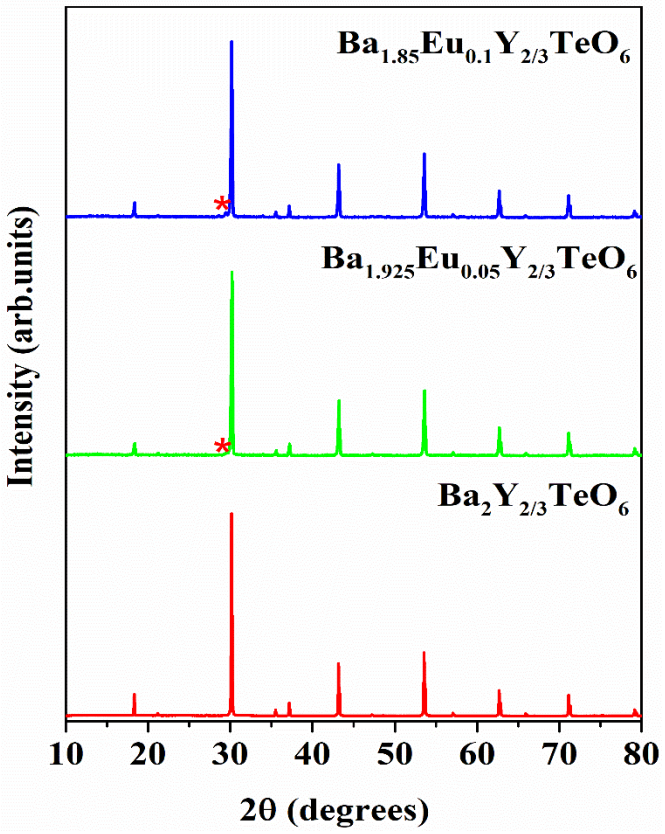

Figure SI 35. Combined XRD pattern of A-site substituted $Ba_2Y_{2/3}TeO_6$: Eu^{3+}.

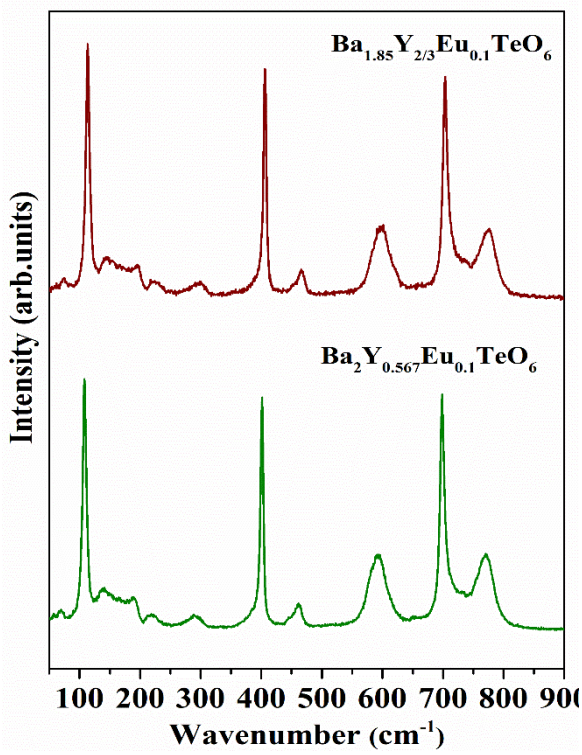

Figure SI 36. Raman spectra of A and B-site substituted $Ba_2Y_{2/3}TeO_6$: Eu^{3+}.

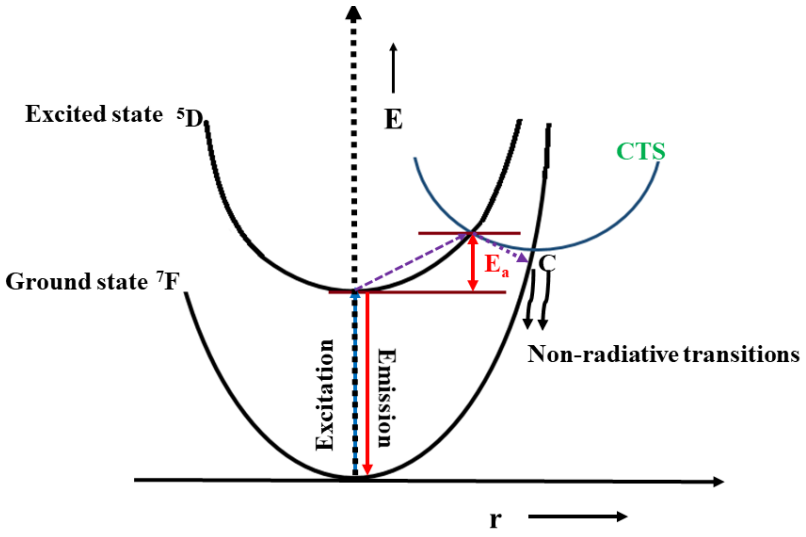

Figure SI 37. Configuration coordinate diagram showing the thermal quenching path of Eu^{3+} emission.

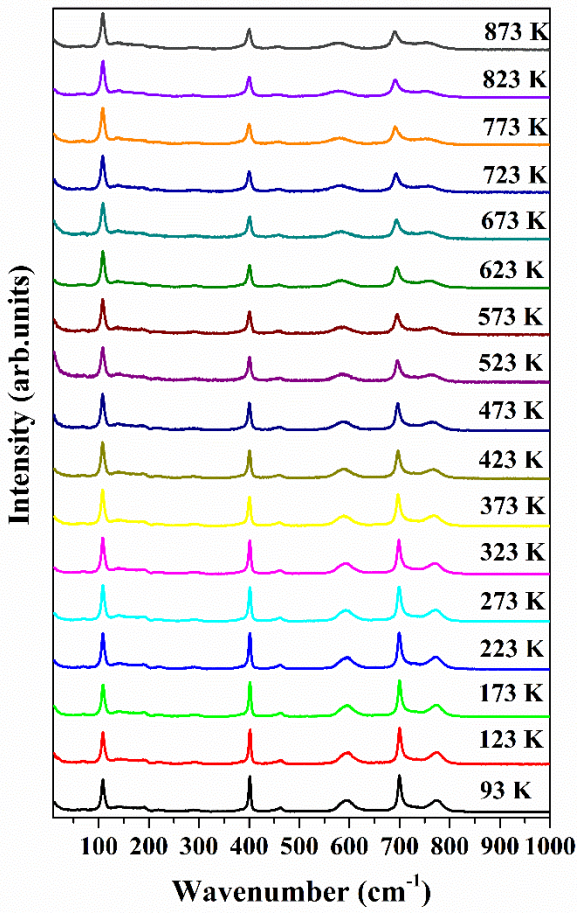

Figure SI 38. Temperature dependent Raman spectra of $Ba_2Y_{2/3}TeO_6$: 10% Eu^{3+} in the range 93 -873 K.

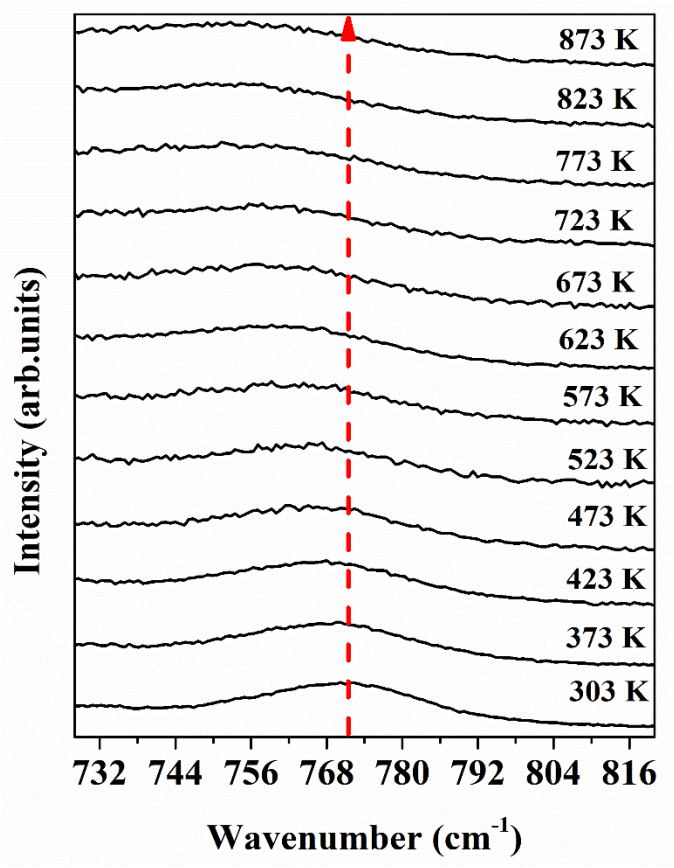

Figure SI 39. Red shift of the symmetric stretching vibration of the B -site octahedron.

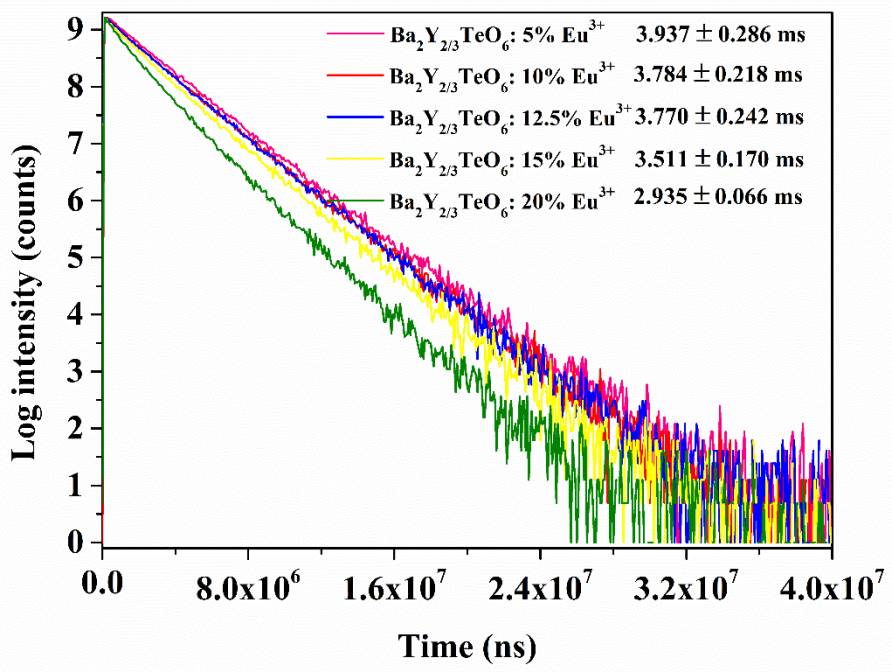

Figure SI 40. PL decay curves of $Ba_2Y_{2/3}TeO_6$: x% Eu^{3+} (x= 5, 10, 12.5, 15, 20%).

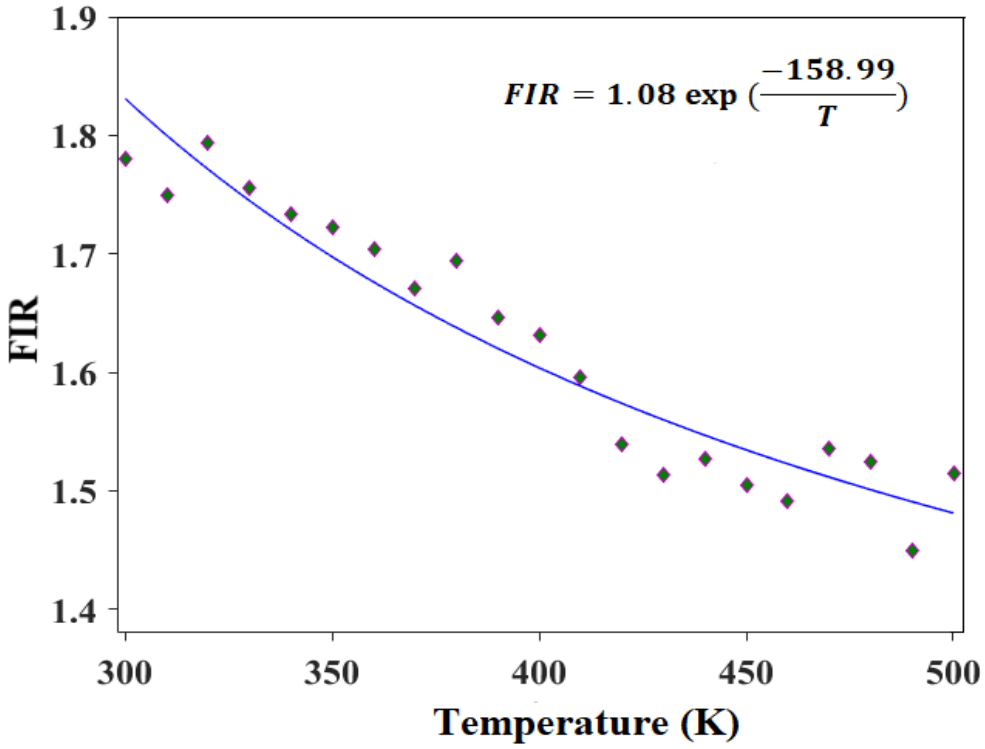

Figure SI 41. Plot of Temperature *vs* FIR of $Ba_2Y_{2/3}TeO_6$: 10% Eu^{3+}.

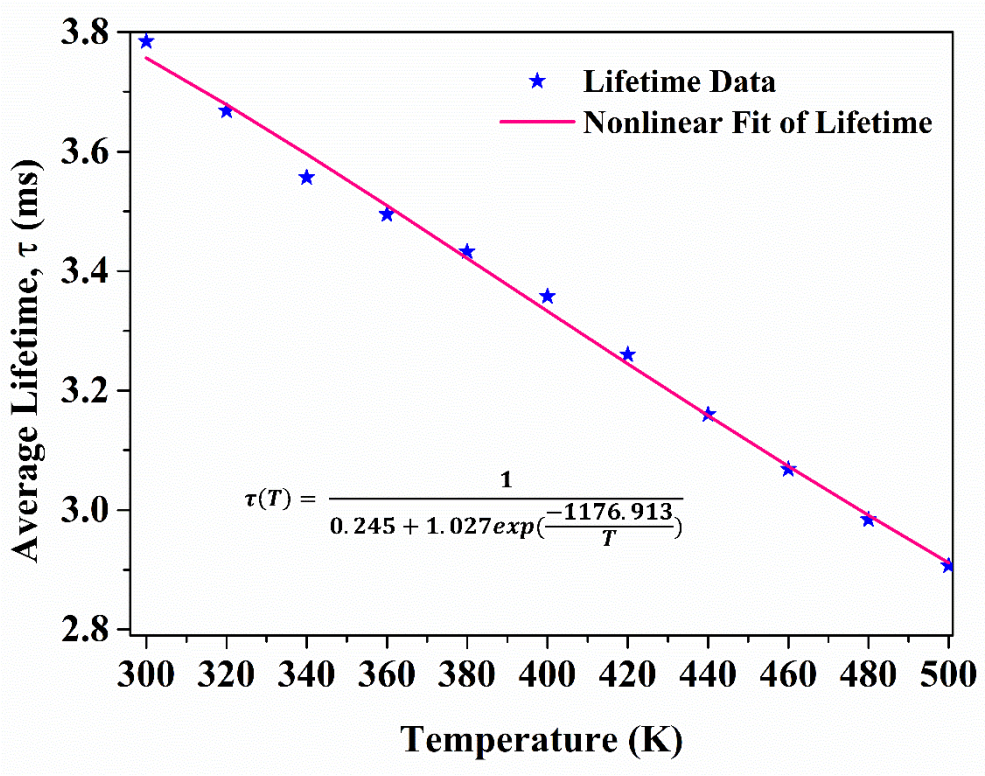

Figure SI 42. Plot of Temperature *vs* Lifetime of $Ba_2Y_{2/3}TeO_6$: 10 %Eu^{3+}.

Judd-Ofelt theory

The Judd-Ofelt and radiative parameters were obtained from the emission spectrum of $Ba_2Y_{2/3}TeO_6$: 10 % Eu^{3+}. Judd and Ofelt separately devised a general theoretical framework for calculating the emission intensities of optical transitions of rare earth ions in specific host materials. W.F Krupke **[64]** proposed a method for calculating the Judd- Ofelt intensity parameters Ω_2, Ω_4 and Ω_6 of trivalent rare earth ions from the emission spectra since the electric dipole transitions $^5D_0 - {}^7F_2$, $^5D_0 - {}^7F_4$ and $^5D_0 - {}^7F_6$ have a direct dependence on the JO parameters. Here, JO parameters are estimated by considering the magnetic dipole transition $^5D_0 - {}^7F_1$ of Eu^{3+} ions as reference.

The rate of magnetic dipole transition is given by **[65-69]**

$$A_{01} = \frac{64\pi^4 \vartheta_1^3 \, n^3 S_{md}}{3h\,(2J+1)} \tag{11}$$

where ϑ_1 is the wavenumber of the corresponding transition, n is the effective refractive index of the phosphor, $S_{md} = 7.83 \times 10^{-42}$ units, which is a constant and independent of the medium, h is Planck's constant and 2J +1 = 1 for $^5D_0$ transitions.

The electric dipole transitions (J=2,4,6) rate can be expressed as

$$A_{0J} = \frac{64\pi^4 \vartheta_J^3}{3h\,(2J+1)} e^2 \frac{n(n^2+2)^2}{9} \sum_{\lambda=2,4,6} \Omega_\lambda \langle {}^5D_0 \left\| U^{(\lambda)} \right\| {}^7F_J \rangle^2 \tag{12}$$

Where A_{0J} is the coefficient of spontaneous emission, e is the charge of electron, Ω_λ (λ= 2,4,6) is the Judd- Ofelt parameters and $\langle {}^5D_0 \left\| U^{(\lambda)} \right\| {}^7F_J \rangle^2$ is the squared reduced matrix element which is independent of the host crystal field environment of Eu^{3+} ions and are 0.00324, 0.00229 and 0.00023 for J = 2,4 and 6 respectively. However, $^5D_0 - {}^7F_6$ transition usually falls in the NIR region and are too weak to be detected. Hence, Ω_6 parameter is omitted here **[65-69]**.

Since the rate of transition from each energy level is directly proportional to integrated emission intensity, ratio of electric dipole to magnetic dipole transition is given as

$$\frac{\int I_J d\vartheta}{\int I_1 d\vartheta} = \frac{A_{0J}}{A_{01}} = \frac{e^2}{S_{md}} \frac{\vartheta_J^3}{\vartheta_1^3} \frac{(n^2+2)^2}{9n^2} \Omega_\lambda \, \langle {}^5D_0 \left\| U^{(\lambda)} \right\| {}^7F_J \rangle^2 \tag{13}$$

The observed fluorescence lifetime is proportional to total transition rate A_T as

$$\frac{1}{\tau_{obs}} = A_T = A_R + A_{NR} \tag{14}$$

where A_R is the radiative transition rate and A_{NR} is the non- radiative transition rate.

Now, the total radiative transition rate, $A_R = \sum_{J=0}^{4} A_{0J} = \frac{1}{\tau_{rad}}$ (15)

Quantum efficiency is related with radiative and non-radiative processes by the relation,

$$\eta = \frac{\tau_{obs}}{\tau_{rad}} = \frac{A_R}{A_R + A_{NR}} \tag{16}$$

Branching ratio gives the percentage of a particular $^5D_0 - {}^7F_J$ emission transition to total radiative transition and is given by

$$\beta_{0J} = \frac{A_{0J}}{\sum A_{0J}} \quad (17)$$

References

64. W.F. Krupke, Phys. Rev., 1966, 145, 325-337.

65. B.R. Judd, Phys. Rev., 1962, 127, 750 – 761.

66. G.S. Ofelt, J. Chem. Phys., 1962, 37, 511 – 520.

67. M.P. Hehlen, M.G. Brik and K.W. Kramer, J. Lumin.,2013, 136, 221 – 239.

68. B.M. Walsh, Advances in Spectroscopy for Lasers and Sensing conference proceedings, 2005, Chapter 21, pp 403 – 433.

69. J.D.L. Dutra, T.D. Bispo and R.O. Freire, J. Comput. Chem., 2014, 35, 772–775.